PNAS

Supplementary Information for

Serine 408 phosphorylation is a molecular switch that regulates structure and function of the occludin α-helical bundle

Atul K. Srivastava[1], Bharat Somireddy Venkata[1], Yan Y. Sweat[2], Heather R. Rizzo[2], Léa Jean-François[2], Li Zuo[2,3], Kathleen W. Kurgan[1], Patrick Moore[1], Nitesh Shashikanth[2], Izabela Smok[1], Joseph R. Sachleben[4], Jerrold R. Turner[2,*], Stephen C. Meredith[1,*]

[1] Department of Pathology, The University of Chicago, Chicago, IL 60637
[2] Laboratory of Mucosal Barrier Pathobiology, Department of Pathology, Brigham and Women's Hospital and Harvard Medical School, Boston, MA, 02115
[3] Anhui Medical University, Hefei, Anhui, China, 230032
[4] Biomolecular NMR Facility, The University of Chicago, Chicago, IL 60637

Jerrold R. Turner or Stephen C. Meredith
jrturner@bwh.harvard.edu or scmeredi@uchicago.edu

This PDF file includes:

Supplementary Information Text

Materials and Methods

Expression of occludin 383-522^{S408A}, 383-522^{S408D}, and 413-522; incorporation of ^{2}H, ^{13}C, and ^{15}N isotopes: Proteins and peptides used in these studies are listed in Table I. Clones for GST-occludin 383-522 wild-type, S408D, and S408A constructs were generated by site-directed mutagenesis as previously described.(1) Recombinant proteins were uniformly labeled with ^{15}N, ^{13}C, and ^{2}H, either alone or in combinations. Small cultures (one colony placed into 10 ml of LB Miller) of *E. coli* (Rosetta (DE3)pLysS bacteria) were grown at 37 °C for 6-8 hours in 250 ml of LB. After centrifugation (2000 x *g* for 10 min at room temperature), bacteria were transferred to M9 minimal medium containing the appropriate isotopes: ^{15}N-NH_4Cl (as only source of nitrogen), ^{13}C-D-glucose (as only source of carbon), and 100% D_2O for deuteration (all from Cambridge Isotopes). Cells were incubated for 12-16 h (overnight) at 37 °C, pelleted (2000 x *g* for 10 min), then added to one liter of fresh minimal media M9 (containing only salts and 1X BME vitamin mix) with the above isotopes. Cell growth was monitored by following OD_{600} until this value reached 0.8-1.2, at which point induction by IPTG (final concentration 1 mM) was started. Cells were then incubated at 25 °C for 16-20 h, and after which they were harvested by centrifugation at 6000 x *g* for 20 min at 4°C.

Expression of occludin 383-412 peptides: Occludin 383-412 peptides were expressed using essentially the same method that was used for occludin 383-522 proteins. The construct was a GST-fusion protein containing a TEV protease cleavage site before the region of our interest. The 383-412 peptides were first purified using a GST column, and then by RP-HPLC, after which they were lyophilized. The lyophilized peptides were redissolved in suitable buffers for experiments or for MTSL labeling at position 409C (as described above).

Purification of occludin 383-522^{S408A}, 383-522^{S408D}, and 413-522: After resuspension of the bacterial pellet in lysis buffer (PBS containing 1mM DTT, 100 µg DNase/ml, 2x Protease Inhibitor (Sigmafast S8820)), bacteria were sonicated using a Branson 250 sonicator with a microtip (pulse setting 10 s on, 1 min off, 20% amplitude, repeated for 15-18 cycles), after which the lysate was clarified by centrifugation in a Sorvall RC-5B centrifuge, 24,000 x *g* at 4 °C for 30 min. The supernatant was harvested for chromatography. The fusion protein was first purified by GSH-Sepharose affinity chromatography (5 ml, Bio-Rad GST Cartridge). The column was equilibrated with PBS (pH 7.4) containing 1 mM DTT. Lysate was loaded onto the column using a peristaltic pump (1 ml/min); the flow-through was collected and re-applied to the column. The column was washed with three solutions in succession (16 column volumes each): PBS, PBS with 0.26 M NaCl, and then 10 mM sodium phosphate (all pH 7.1 with 1 mM DTT). After washes, 0.03 mg

HRV 3C Protease (Pierce) in 5 ml of 10 mM sodium phosphate (pH 7.1 with 1 mM DTT) was added and the column was capped and incubated for 16-20 h at 4°C. Occludin proteins liberated by the protease were eluted from the column using 10-15 ml of 10 mM sodium phosphate (pH 7.1 with 1 mM DTT). Further purification was performed using a Äkta pure FPLC system equipped with a HiLoad 16/600 Superdex 75 pg column. Eluent was 10 mM sodium phosphate (pH 7.1 with 1 mM DTT); flow rate was 1 ml/min; effluent was monitored as A_{280}, A_{230}, and A_{220}. Fractions containing the fusion protein were identified by SDS-PAGE stained using Coomassie blue. Purity was assessed by SDS-PAGE. After purification, protein was concentrated using Millipore Amicon Ultrafiltration (10 kD MWCO) to a volume of ~ 0.5-0.6 ml. Protein concentration was estimated using the extinction coefficient of 20400 M^{-1} cm^{-1} (using the equation ε_{280nm} = 5500*W + 1490*Y+ 125*C, where W, Y and C are the numbers of Trp, Tyr and Cys residues in each peptide or protein.(2) Typical final protein concentrations were ~0.2 mM.

CD Spectroscopy: Protein and peptide concentrations were estimated from UV spectra as described above. CD spectra were measured using a Jasco J-1500 spectropolarimeter. Path length was 1 mm. Spectra were measured from 280-180 nm. Mean residue ellipiticity was calculated from the concentration, path length, and a calculated mean residue molecular weight of 116.94. α-helical content was estimated using the equation % helix = 100 x (θ_{222nm} – 3000)/-39000.(3) To assess thermal denaturation and renaturation, temperature was varied from 26 to 80 °C (forward and reverse) by 2 °C intervals, with a thermal equilibration period of 3 min. between each temperature. Curves were constructed using the ellipticity at 222 nm and 208 nm.

NMR assignments: Initial experiments indicated that better peak resolution was obtained using TROSY sequences e.g., ^{15}N-TROSY rather than ^{1}H^{15}N-HSQC. In addition, samples for peak assignments were generally deuterated, i.e., labeled with ^{2}H, ^{13}C, and ^{15}N. From mass spectrometry, the deuteration level of the final product averaged ~ 65%. In some experiments protein was expressed in bacteria grown using perdeuterated ^{13}C-D-glucose as only source of carbon. This perdeuterated protein yielded sharper peaks than were obtained with partially deuterated protein. In general NMR spectra were obtained using either a 500- or 600-MHz NMR Bruker spectrometer equipped with TopSpin software. The following types of spectra were acquired and used to obtain peak assignments: 1) ^{15}N-TROSY (trosyetfpf3gpsi): 2D H-1/X correlation via TROSY, using Echo/Antiecho gradient selection.(4-10) 2) HNCO (trhncoetgp3d): TROSY-HNCO 3D sequence with inverse correlation for triple resonance via TROSY and inept transfer steps.(11, 12) 3) HNcoCACB (trhncocacbgp2h3d): TROSY-HNcoCACB 3D sequence with inverse correlation for triple resonance via TROSY and inept transfer steps (42-44).(11-14) 4) HNCACB (trhncacbgp2h3d): TROSY-HNCACB 3D sequence with inverse correlation for triple

resonance TROSY and inept transfer steps (42-44). 5) HNcaCO (trhncacogp2h3d): TROSY-HNCACO 3D sequence with inverse correlation for triple resonance via TROSY and inept transfer steps.(13) Other experiments used in some cases included: HNCA (trhncaetgp3d)(11-14); HNcoCA (trhncocaetgp3d, (11-14); ^{15}N-HSQC (hsqcetfpf3gpsi)(13) and ^{13}C-HSQC (hsqcetfpgpsi2).(15-19) NMR spectra were processed using NMRPipe,(20) and imported into CARA(21) for assignments.

Dynamics of occludin 383-522^{S408A} and *383-522^{S408D} as measured by NMR*: To assess the conformational dynamics of residues in occludin 383-522^{S408A} and 383-522^{S408D} by NMR, the following experiments were performed using 2D H-1/X correlation via TROSY and inept transfer: 1) Measurement of ^{15}N T_1 and T_2 relaxation times (trt1etf3gpsi and trt2etf3gpsi), respectively.(22) 2) Heteronuclear ^{1}H-^{15}N NOEs (trnoef3gpsi) were measured as 2D H-1/X correlation via TROSY and inept transfer, under unsaturated and saturated conditions. 3) Water-amide proton exchange rates were measured using the Phase-Modulated CLEAN chemical EXchange (CLEANEX-PM) method with a Fast-HSQC (FHSQC) detection scheme.(23, 24)

Spectra were processed using NMRPipe and imported into NMRView for measurement of peak volumes and kinetics analysis. For calculation of R_1, the reciprocal of T_1, the decline in volume for each peak (assignments obtained as described above) was assessed as a function of parameter d7 (Bruker pulse sequence trt1etf3gpsi for measuring ^{15}N T_1 relaxation times), which was varied from 10 to 2000 ms. For calculation of R_2, the reciprocal of T_2, the decline in peak volume was assessed as a function of either parameter d20 or d31 (Bruker pulse sequence trt2etf3gpsi for measuring ^{15}N T_2 relaxation times), which was varied from 20 to 240 ms. In both cases, data were analyzed using the equation of a mono-exponential decay, i.e.,

$$V_t = Ae^{-kt} + V_{eq}$$

where V_t = peak volumes at different values of d7 or d20, k = rate constant (R_1 or R_2), V_{eq} = peak volume extrapolated to infinite time, and A is a parameter. For most residues, T_2 relaxation was complete after 80-100 ms because of the large size (for NMR) and elongated structure of these proteins; that is, analysis of decay curves was often based on only 4 or 5 points. Thus, R_2 measurements are considered as approximate and were used solely to compare with the slower relaxing residues in the unstructured parts of these proteins. For Heteronuclear NOEs,(19, 25) similar procedures were followed. Spectra were obtained using Bruker pulse sequence trnoef3gpsi; the spectra were split into reference and proton-saturated components, and the volumes measured as described for T_1 / T_2 measurements. Similar procedures were followed for

CLEANEX-PM, except that ^{15}N resonances were acquired from $^{1}H^{15}N$-HSQC spectra rather than from NTROSY experiments.

Chemical Shift Perturbations: Chemical Shift Perturbations (CSPs) between proteins were calculated using the following equation(26):

$$CSP = \sqrt{\left(\partial_{OCCA,H} - \partial_{OCCD,H}\right)^2 + 0.15 * \left(\partial_{OCCA,N} - \partial_{OCCD,N}\right)^2}$$

The above equation was used for comparing occludin 383-522^{S408A} and 383-522^{S408D}; similar calculations were made to compare occludin 383-522^{S408D} or 383-522^{S408A} to occludin 413-522.

Paramagnetic Relaxation Enhancement (PRE) experiments: For PRE experiments,(27, 28) selected cysteine residues in occludin proteins or peptides were labeled with *S*-(1-oxyl-2,2,5,5-tetramethyl-2,5-dihydro-1H-pyrrol-3-yl)methyl methanesulfonothioate (MTSL) or its diamagnetic variant 1-acetyl-2,2,5,5-tetramethyl-3-pyrroline-3-methyl-methanethiosulfonate (MTS) as follows.(29) Approximately ~5-6 mg of protein was dissolved in 50 mM Tris, 50 mM NaCl, also containing 20 mM DTT, pH 7.8. Prior to reaction with MTSL, DTT was removed using a desalting column. Protein was then incubated at room temperature for 30 minutes with 70 mM MTSL or MTS dissolved in 50 µL of DMS0. The MTSL- or MTS-protein or peptide mixture was incubated overnight at 4°C and purified by HPLC.

We examined PRE effects of MTSL-labeled cysteine in occludin in two ways. The various constructs used for these experiments are listed in Table 1.

Initial studies were carried out using occludin 383-522^{S408A} or 383-522^{S408D} containing a single MTSL- or MTS-label, i.e., with the unstructured domain as part of the entire occludin protein ("in cis" with the α-helical bundle, Table I). For these experiments, we used two sets of constructs, each with a single labeled cysteine residue at different positions. First, we labeled C409 in constructs of occludin 383-522^{S408A} or 383-522^{S408D}, in which the other cysteine residue, C500, had also been mutated to Ser, so that C409 was the only cysteine residue present. In another set of experiments, we expressed two versions of occludin 383-522^{S408A} or 383-522^{S408D}, in which A383 was mutated to cysteine, and the two other cysteine residues (C409 and C500) were mutated to serine, so that C383 would be the only cysteine residue (Table I).

To assess spin-labeling, MTSL-labeled peptides from the unstructured domain, occludin 383-412^{S408A} or 383-412^{S408D}, were added to occludin protein containing only the α-helical bundle, occludin$^{413-522}$. That is, in this second group of experiments, the labeled peptides were added to

unlabeled protein *in trans*, and the unlabeled protein contained only the α-helical bundle. In addition, these expressed peptides contained a SGGGG-leader sequence.

Furthermore, we performed two variations of the PRE experiments. The usual method for reducing MTSL to its diamagnetic form is to incubate the protein with ascorbate. This procedure was followed for experiments in which MSTL-labeled 383-412 peptides were added to occludin 413-522. For examining PRE of occludin 383-522^{S408A} or 383-522^{S408D} labeled at C409 or C383 with MTSL, however, we observed that a small amount of the MTSL-labeled protein was lost to precipitation or other causes over the course of this somewhat lengthy experiment, which could confound the interpretation of PRE experiments. Accordingly, we took the alternate approach of comparing MTSL-occludins (paramagnetic) with MTS-occludins (diamagnetic). The advantage of this approach, aside from avoiding subquantitative recoveries after incubation of the protein with ascorbate, is that we were able to track losses of protein with serial NTROSY experiments. Thus, we documented that the NMR signal of MTSL- and MTS-occludin 383-522^{S408A} or 383-522^{S408D} remained constant for the duration of the experiments. PRE effects were then calculated as the volume ratios of peaks from MTSL- and MTS-labeled proteins.

For experiments in which MTSL- or MTS-labeled peptides were added to occludin proteins, the concentration of ^{15}N-occludins was 100 μM and the concentration of the peptides was 200 μM in all cases. Buffer was 10 mM sodium phosphate, pH 7.1, containing 8% (v/v) D_2O (which contained 1% (w/v) DSS). Temperature was 25° C. For experiments using MTSL- or MTS-labeled occludin proteins, the protein concentration was 250 μM, buffer was 10 mM sodium phosphate, pH 7.1, containing 8% (v/v) D_2O (which contained 1% (w/v) DSS). Temperature was 25° C. Spectra were acquired and processed as described above. Results are reported as ratios of MTSL to MTS peak volumes.

Microscale thermophoresis: Recombinant occludin proteins were expressed in Rosetta2 (DE3)pLysS bacteria (Novagen) and purified on GST columns and 3C protease was used to remove GST tags, as above. Occludin 383-412^{S408} and 383-412^{S408P} peptides were synthesized commercially (ThermoFisher). For microscale thermophoresis, His-tagged occludin constructs were labeled using MonolithNT His-Tag Labeling Kit (NanoTemper). Microscale thermophoresis was performed using a Monolith NT.115 (NanoTemper). Data were analyzed by MO Affinity Analysis software.

Mice, intravital imaging and FRAP: 7–12-wk-old mice maintained on a C57BL/6 genetic background were used for all experiments. EGFP-occludin^{S407A} transgenic mice were created as previously described for villin-EGFP-occludin (wildtype) mice.(30) *Ocln$^{f/f}$ x* villin-Cre mice(31)

were crossed with villin-EGFP-occludin(30) or EGFP-occludin^{S407A} mice so that only EGFP-occludin or EGFP-occludin^{S407A} was expressed within the intestinal epithelium. FRAP analysis was performed as reported previously.(1, 32) Briefly, mice were anesthetized and the abdomens were opened by a midline incision. Electrocautery used to open a 2-cm loop of jejunum along the antimesenteric border. The abdominal cavity was closed beneath the externalized jejunal loop while taking care to protect the neurovascular supply. The exposed mucosal surface was placed against the coverslip bottom of a 35-mm Petri dish containing 0.15 ml HBSS, with the body of the mouse over the jejunum, and both were placed within a 37°C heated enclosure. Imaging was performed using an inverted DM6000 microscope (Leica) equipped with a HC PL APO 100x/1.40 OIL CS2 objective (Leica), 488 nm argon laser with Borealis illumination (Andor), 405, 488, 588, 660 multi-bandpass dichroic and 540/50 emission filter (Semorck), CSU-X1 spinning disk (Yokogowa), Zyla PLUS 4.2 CMOS camera (Andor), and micropoint FRAP/photoablation system (Andor). Raw data were aligned and mean fluorescence of background, whole-field, and bleached regions were quantified over time using ImageJ. Background fluorescence was subtracted from bleached regions and whole-field fluorescence at each time point. Bleached region and whole-field data were normalized to their respective prebleach intensities, and fluorescence recovery within bleached regions relative to whole-field intensity was plotted over time. After fitting data to $f(x) = y_0 + a(1 – e^{-bx})$, mobile fractions and halftimes of recovery were calculated as $(a)/(1 - y_0)$ and $\ln(2)/b$, respectively. All experiments were performed in an Association of Assessment and Accreditation of Laboratory Animal Care–accredited facility under protocols approved by The Institutional Animal Care and Use Committee.

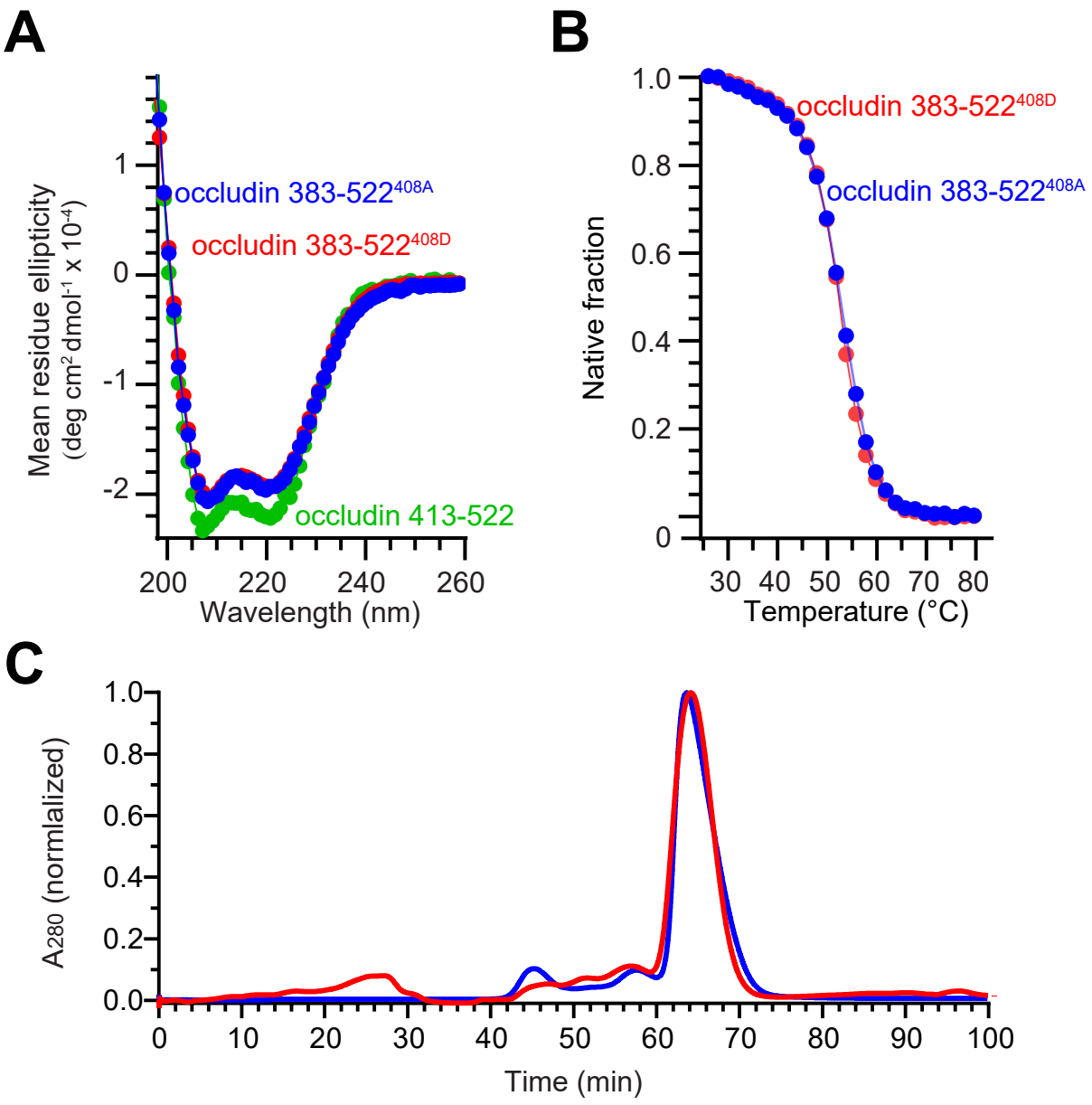
A
Mean residue ellipticity
(deg cm^2 dmol^{-1} x 10^{-4})
occludin 383-522^{408A}
occludin 383-522^{408D}
occludin 413-522
Wavelength (nm)
B
Native fraction
occludin 383-522^{408D}
occludin 383-522^{408A}
Temperature (°C)
C
A$_{280}$ (normlalized)
Time (min)

Fig. S1. S408 pseudophosphorylation does not cause global structural changes within the occludin cytoplasmic tail. ***A.*** Circular dichroic spectroscopy curves of occludin 383-522^{S408A} (blue), 383-522^{S408D} (red), and 413-522 (green). α-helical content was estimated using the equation % helix = 100 x (θ_{222nm} – 3000)/-39000 (3). The apparent helical content of 383-522^{S408A} and 383-522^{S408D} were both 56.6%. Occludin 413-522 had a slightly higher helical content (63.4%), presumably due to removal of the unstructured domain. ***B.*** Melting curves depicting occludin 383-522^{S408A} (blue) and 383-522^{S408D} (red), both of which showed cooperative and reversible thermal melting behavior) and similar midpoints at ~ 50°C. ***C.*** Size exclusion chromatography of occludin 383-522^{S408A} (blue) and 383-522^{S408D} (red) using a 16/100 Superdex 75 PG column in buffer containing 1.0 mM DTT (1, 33-35).

Srivastava et al., Figure S2

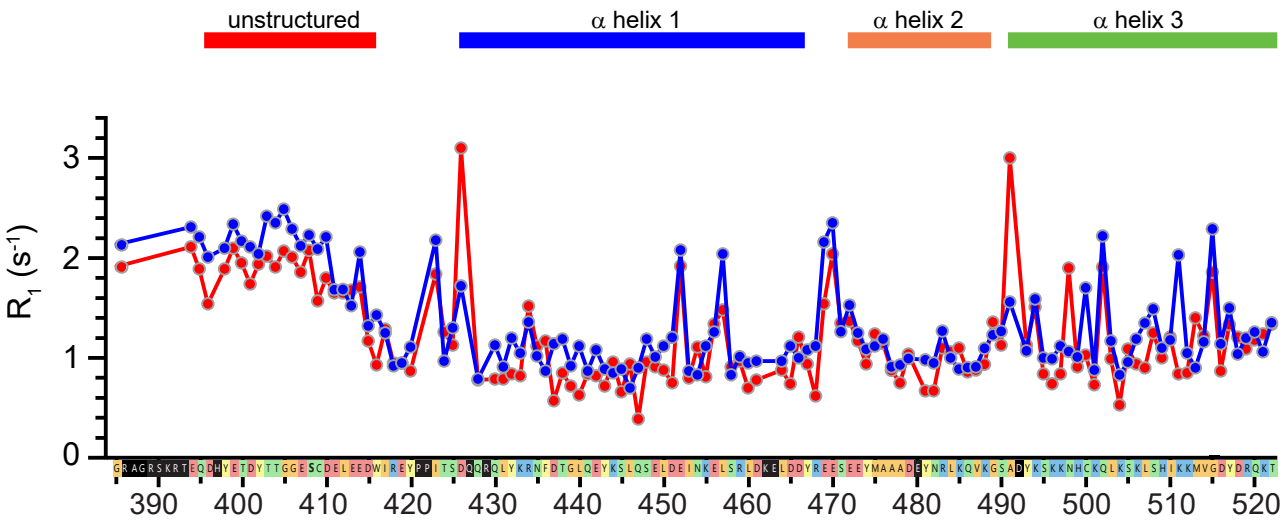

Fig. S2. R_1 (T_1) measurements. ^{15}N-labeled occludin 383-522^{S408A} (blue) and occludin 383-522^{S408D} (red) spectra were processed using NMRPipe and imported into NMRView for measurement of peak volumes and kinetics analysis. For calculation of R_1, the decline in volume for each peak (assignments obtained as described) was assessed as a function of parameter d7 (Bruker pulse sequence trt1etf3gpsi for measuring ^{15}N T_1 relaxation times), which was varied from 10 to 2000 ms. Data were analyzed using the equation of a mono-exponential decay, i.e.,

$$V_t = Ae^{-kt} + V_{eq}$$

where V_t = peak volumes at different values of d7 or d20, k = rate constant (R_1 or R_2), V_{eq} = peak volume extrapolated to infinite time, and A is a parameter.

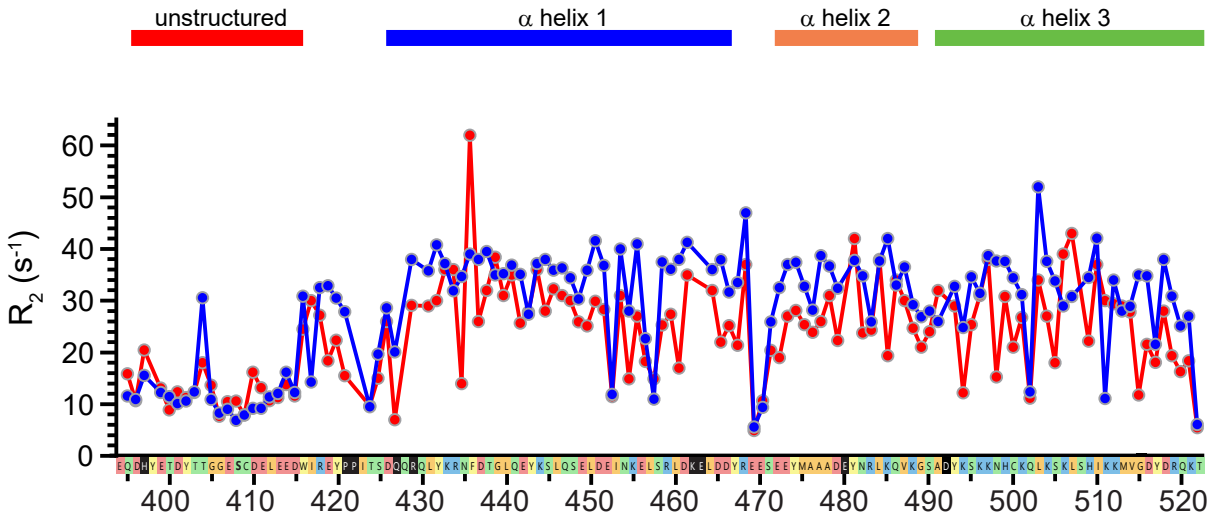
unstructured
α helix 1
α helix 2
α helix 3
R2 (s-1)
0
10
20
30
40
50
60
400
410
420
430
440
450
460
470
480
490
500
510
520

Fig. S3. R_2 (T_2) measurements. As for measurement of R_1, the decline in ^{15}N-labeled occludin 383-522^{S408A} (blue) and occludin 383-522^{S408D} (red) peak volume was assessed as a function of parameter d7 (Bruker pulse sequence trt2etf3gpsi for measuring ^{15}N T_2 relaxation times), which was varied from 20 to 240 ms. Calculations of R_2 were as described for R_1. For most residues, relaxation was complete after 80-100 ms because of the large size (for NMR) and elongated structure of these proteins; that is, analysis of decay curves was often based on only 4 or 5 points. Thus, R_2 measurements are considered as approximate and were used solely to compare with the slower relaxing residues in the unstructured parts of these proteins.

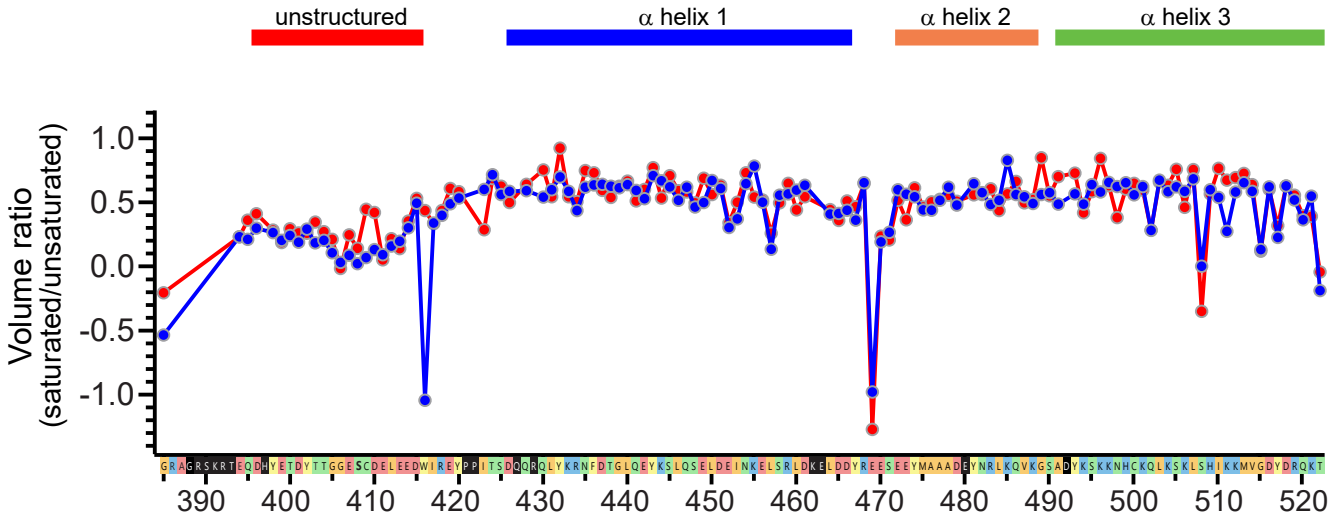
unstructured
α helix 1
α helix 2
α helix 3
Volume ratio
(saturated/unsaturated)
1.0
0.5
0.0
-0.5
-1.0
390
400
410
420
430
440
450
460
470
480
490
500
510
520

Fig. S4 Heteronuclear NOEs. Spectra of ^{15}N-labeled occludin 383-522^{S408A} (blue) and occludin 383-522^{S408D} (red). Procedures used for measuring heteronuclear NOEs were similar to those followed for R_1 and R_2.(19, 25) Spectra were obtained using Bruker pulse sequence trnoef3gpsi; the spectra were split into reference ("Unsaturated") and proton-saturated ("Saturated") components, and the volumes measured as described for R_1 / R_2 measurements. Data are reported as the ratio of Saturated to Unsaturated peak volumes.

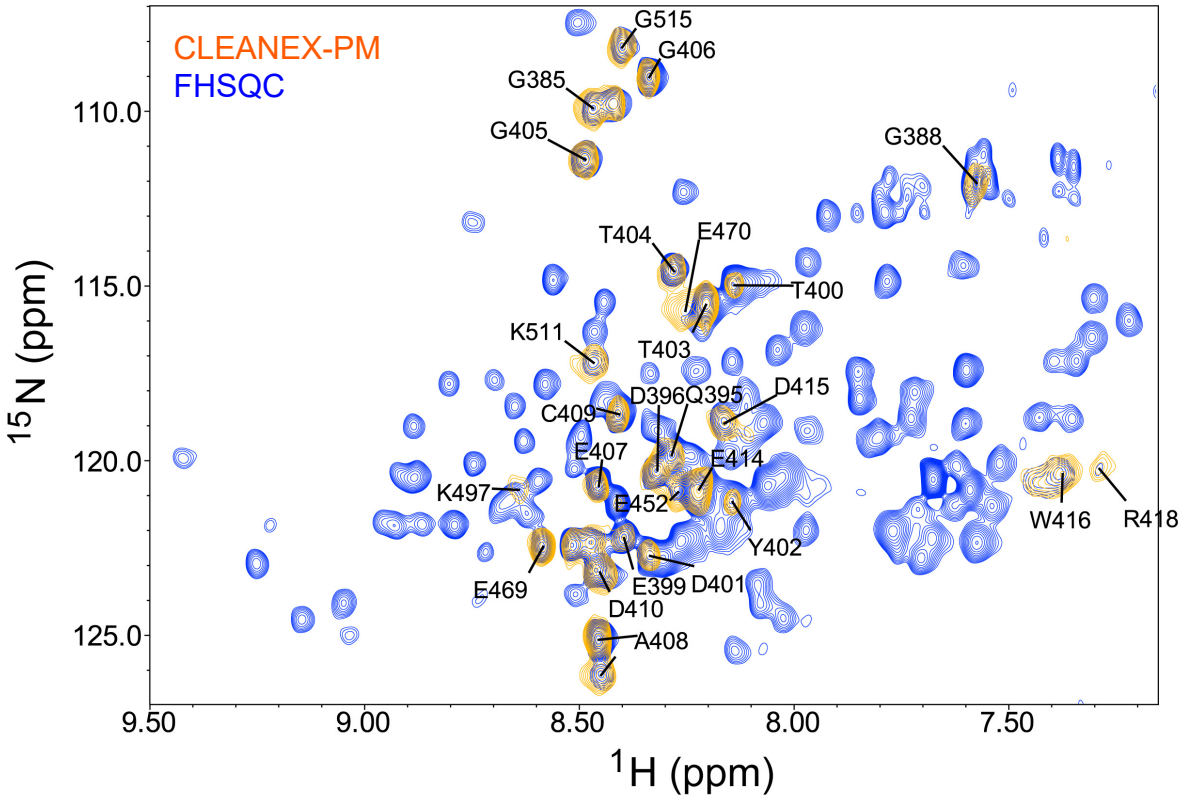
CLEANEX-PM
FHSQC
G515
G406
G385
G405
G388
T404
E470
T400
K511
T403
D396
Q395
D415
C409
E407
E414
K497
E452
Y402
W416
R418
E469
E399
D401
D410
A408
110.0
115.0
120.0
125.0
15N (ppm)
9.50
9.00
8.50
8.00
7.50
1H (ppm)

Fig. S5. CLEANEX-PM data. Water-amide proton exchange rates of on ^{15}N-labeled occludin 383-522^{S408A} and 383-522^{S408D} were measured using the Phase-Modulated CLEAN chemical EXchange (CLEANEX-PM, orange)(23, 24) method with a Fast-HSQC (FHSQC, blue) detection scheme. Mixing times (n = 8 independent experiments) were varied from 0.01 to 0.3 s. Results were similar at all mixing times. Results for ^{15}N-labeled occludin 383-522^{S408A}. are shown and are essentially identical to results using ^{15}N-labeled occludin 383-522^{S408D}. These data all indicate that the unstructured domain is generally more solvent exposed than residues within the α-helices. Some residues at bends in the α-helices or turns between helices were also relatively solvent exposed.

Table S1. Proteins and peptides

Name	Residues	Alterations from WT Sequence
Occludin 383-522^{S408A}	383-522	S408A
Occludin 383-522^{S408D}	383-522	S408D
Occludin 413-522	413-522	N-terminal extension GPLGS–
Occludin 383-522^{S408A}-C409-MTSL/MTS	383-522	S408A, C500S, MTSL or MTS at C409
Occludin 383-522^{S408D}-C409-MTSL/MTS	383-522	S408D, C500S, MTSL or MTS at C409
Occludin 383-522^{S408A}-C383-MTSL/MTS	383-522	S408A, A383C, C409S, C500S, MTSL or MTS at C383
Occludin 383-522^{S408D}-C383-MTSL/MTS	383-522	S408D, A383C, C409S, C500S, MTSL or MTS at C383
Occludin 383-412^{S408D}-C409-MTSL/MTS	383-412	SGGGG-leader, S408A, C500S, MTSL or MTS at C409
Occludin 383-412^{S408D}-C409-MTSL/MTS	383-412	SGGGG-leader, S408D, C500S, MTSL or MTS at C409
Occludin 383-412^{S408P}	383-412	Phosphoserine at S408
Occludin 383-412^{S408}	383-412	None

Table S2. Chemical shifts for occludin 383-522^{S408A}

Residue	H	N	CO	CA	CB
A387	7.6060	122.72	179.15	54.151	17.028
G388	7.6360	112.33			
S390	7.4630	114.75		60.959	62.464
T393	7.6000	120.74	177.99	59.669	70.268
Y398	8.0200	121.85	175.63	57.641	37.925
E399	8.2950	122.68	176.34	56.086	29.570
T400	8.0660	115.58	174.09	61.533	69.416
D401	8.2520	123.18	176.26	53.958	40.764
Y402	8.0790	121.27	175.42	57.663	57.663
T404	7.7160	121.16	179.24	63.262	70.350
G405	8.2500	109.48		44.691	
E407	8.1650	122.68	176.53	56.158	29.355
A408	8.3650	125.52	177.72	52.408	18.373
C409	7.8460	126.17	181.54	57.233	
D410	8.3730	123.54	176.20	54.137	40.614
E411	8.3130	121.59	176.36	56.229	29.355
L412	8.2130	123.27	177.24	54.382	41.265
E413	8.2200	122.31	175.20	56.014	29.427
E414	7.6580	118.39	175.50	57.591	30.000
D415	7.9570	115.26	172.71	55.584	38.098
W416	7.6610	122.85	177.22	60.479	30.287
I417	8.3970	119.82	177.83	66.765	37.436
R418	8.3230	118.55	179.45	59.024	31.361
E419	7.7300	122.39	178.35	61.031	30.966
I423	8.4290	124.12	177.33	61.470	37.599
S425	7.2100	115.83	174.09	57.233	66.621
Q428	7.7200	119.72	179.61	59.367	31.176
R429	8.0560	119.98	178.38	58.711	28.144
Q430	7.9390	117.19	178.88	58.164	27.277
L431	7.5960	122.51	178.85	57.949	40.606
Y432	8.7950	122.11	178.18	60.492	35.725
K433	8.5140	119.66	178.23	58.863	30.756
R434	8.1470	120.10	179.51	59.107	28.638
N435	8.4440	119.58	178.82	55.433	37.158
F436	9.0570	124.87	175.54	60.981	38.007
D437	8.7460	120.87	180.45	57.519	39.460
T438	8.3990	115.80	180.48	65.546	68.269
G439	8.1760	112.89		46.698	
L440	8.9320	124.58	178.92	57.318	39.944
Q441	7.2890	117.65	179.02	58.236	27.205
E442	8.0620	119.64	178.37	58.881	28.280
Y443	8.8340	120.81	176.26	61.088	37.814

K444	8.7080	118.25	180.33	59.239	31.218
S445	7.7350	115.29	180.35	60.959	62.464
L446	7.9930	124.60	179.46	57.236	41.829
Q447	8.8080	119.48	178.84	57.810	27.324
S448	7.7280	113.45	178.85	61.246	62.464
E449	7.9880	124.04	179.44	59.203	29.127
L450	8.4940	121.09	178.10	57.236	41.911
D451	8.3540	118.95	178.23	57.233	41.538
E452	8.1650	119.45	179.45	59.433	31.000
I453	7.2770	119.28	177.77	64.120	36.912
N454	7.3570	117.32	178.61	56.086	37.668
K455	8.6480	122.94	179.87	59.168	31.433
E456	8.0870	122.14	177.48	57.804	29.208
L457	8.2460	120.64	178.98	58.219	40.846
S458	7.8350	113.30	178.98	61.031	62.464
L460	8.2200	123.00	176.34	54.368	41.092
D461	7.5170	125.12	174.85	58.618	38.577
L464	8.1080	117.77	178.65	57.233	40.105
D465	7.2180	116.89	177.22	55.584	40.750
D466	7.6600	118.94	176.95	54.868	40.821
Y467	7.5360	119.34	175.81	56.373	39.531
E469	8.5860	124.00	176.09	57.233	29.045
E470	8.1280	116.38	176.22	56.373	27.420
E471	7.9120	116.61	175.06	57.949	65.617
E472	9.1450	123.28	179.62	59.203	28.553
E473	9.2960	120.25	179.15	59.557	26.750
Y474	7.6890	122.32	176.59	61.389	38.170
M475	8.0740	117.49	178.82	58.164	31.218
A476	7.9540	121.13	180.73		17.313
A477	7.6030	123.19	179.20		16.923
A478	8.8310	122.26	180.47	54.626	16.499
A479	7.9740	119.31	179.23	57.072	40.108
Y481	8.8620	122.06	177.09	61.246	38.170
N482	8.3850	116.57	178.21	55.871	37.668
R483	8.0690	122.28	179.61	59.454	29.140
L484	8.2440	121.39	179.31	57.233	40.939
K485	8.4180	120.58	180.28	59.121	30.520
Q486	7.7160	119.61	179.59	57.973	26.832
V487	7.8770	122.32	179.88	66.276	30.593
K480	7.9340	120.69	176.23	58.055	28.717
G489	7.3300	103.27		44.261	
S490	7.7560	113.73		61.318	62.464
Y483	7.6230	121.76	177.39	61.604	38.886
K494	7.9950	118.74	179.68	59.598	31.361
S495	8.5020	115.27	179.72	60.959	62.321

K496	7.9290	124.90	178.72	59.677	31.978
K497	8.5370	121.31	179.84	59.383	31.075
N498	8.1940	119.22	177.64	55.925	37.650
H499	8.5910	122.11	177.75	59.024	29.928
C500	8.5050	118.22	176.11	57.663	39.388
K501	8.4400	122.82	176.61	56.174	29.208
Q502	8.2080	120.28	175.75	55.799	28.710
L503	8.1790	121.35	175.98	54.300	40.532
K504	8.3060	121.92	176.34	56.174	29.289
S505	8.0270	114.89	174.09	61.246	69.416
K506	7.9880	126.20	178.11	59.107	31.082
L507	8.5090	118.14	179.21	57.663	39.316
S508	7.7660	114.27	179.22	61.318	62.536
I510	7.8370	119.66	180.35	57.646	39.863
K511	8.7860	120.76	179.13	56.990	39.863
M513	8.2340	117.94	181.00	57.233	33.798
V514	8.4770	121.99	177.11	66.602	30.919
G515	8.4280	107.84		46.841	
D516	8.7280	122.26	178.73	56.516	39.746
Y517	7.5400	121.75	178.12	60.816	38.743
D518	8.6530	120.57	178.98	56.337	38.970
R519	7.7860	118.62	177.45	57.734	29.283
Q520	7.5040	117.76	176.21	55.799	28.137
K521	7.5070	121.28	176.09	55.838	31.361
T522	7.6000	120.96	179.36	62.966	70.347

* Protein at 180 μM, 25 °C, 10 mM sodium phosphate, pH 7.10, containing D_2O (10% volume) with 0.1% DSS.

Table S3. Chemical shifts for occludin 383-522^{S408D}

Residue	H	N	CO	CA	CB
K391	8.0250	126.02	178.23	29.287	31.218
R392	8.5370	118.10	179.21	57.796	39.277
T393	7.8170	114.53	182.55	61.570	62.932
Q395	8.1705	120.45	120.18	55.740	28.77
D396	8.1221	121.58	121.51	54.300	40.69
H397	8.3090	122.57	176.38	56.328	29.696
Y398	8.0398	121.96	174.77	56.310	29.68
E399	8.2950	122.97	175.76	61.740	69.52
T400	8.1072	116.41	174.87	53.970	40.64
D401	8.2338	123.43	174.09	59.200	38.66
Y402	7.5160	125.03	180.41	59.203	36.656
T404	8.2060	115.03	175.30	61.757	69.482
G405	8.4080	111.93	174.75	45.093	
G406	8.2575	109.79	174.75	44.830	
E407	8.4257	121.27	174.39	56.530	29.41
D408	8.4168	121.87	176.45	54.230	40.62
C409	8.2431	119.94	179.73	58.360	28.09
D410	8.4159	124.12	174.31	54.600	40.99
E411	8.3260	122.13	176.19	56.380	29.53
L412	8.2224	123.79	176.28	54.640	41.60
E413	8.2044	123.30	177.13	56.430	29.44
E414	8.1156	121.67	176.86	56.320	28.95
D415	8.0612	120.57	179.54	54.720	40.01
W416	7.4638	121.21	177.47	58.190	28.43
I417	7.5648	120.71	177.25	63.260	36.97
R418	7.3558	119.55	177.24	58.020	29.02
E419	7.6023	118.86	177.70	57.600	30.20
Y420	8.0401	115.67	176.45	55.740	38.40
I423	8.4125	124.51	176.29	61.740	37.86
T424	8.6477	113.91	177.29	61.440	70.28
S425	7.2007	116.09	174.41	57.600	66.98
D426	9.1380	122.31	178.96	65.607	
Q428	7.4910	122.70	177.12	57.740	
Q430	7.9398	117.60	177.98	60.980	30.46
L431	7.5788	122.97	178.89	66.940	37.64
Y432	8.7652	122.59	178.79	57.340	31.56
K433	8.5362	120.22	178.12	59.240	31.17
R434	8.1386	120.55	178.07	59.370	29.02
N435	8.3938	119.91	179.47	55.710	37.27
F436	9.0421	125.25	178.72	61.290	38.31
D437	8.7660	121.26	175.49	57.580	39.63
T438	8.3415	116.18	180.44	65.710	68.59

G439	8.1578	113.07	177.75	47.030	
L440	8.9451	124.83	175.23	57.650	40.24
Q441	7.2337	117.87	178.86	58.440	27.33
E442	7.4373	122.04	178.93	59.120	28.60
Y443	8.8284	121.15	178.42	61.510	38.09
K444	8.6985	118.52	176.22	59.660	31.25
S445	7.6775	115.61	180.26	61.150	62.58
L446	7.9810	124.92	176.94	57.430	41.96
Q447	8.7909	119.79	178.54	58.020	27.53
S448	7.7490	113.68	176.32		
E449	7.9837	124.26	176.97		
L450	8.3982	121.04	179.26	57.500	42.03
D451	8.3495	119.28	178.03	59.700	31.07
E452	8.1780	119.90	178.06	58.860	28.09
I453	7.2512	119.54	179.10	57.650	42.48
N454	7.3010	117.88	177.42	57.430	41.70
K455	8.6178	123.30	178.39	57.930	31.30
E456	8.0697	122.49	179.81	58.270	27.50
L457	8.2237	121.05	177.93	58.100	40.86
S458	7.8185	113.68	178.95	61.060	62.75
R459	7.4797	123.26	176.76	59.134	28.800
L460	7.8797	119.99	179.73	61.440	38.24
D461	8.7916	121.26	180.41	59.507	31.543
K462	8.6560	122.95	179.86	57.945	29.007
E463	8.0770	122.08	178.82	59.460	29.01
L464	8.1278	118.18	178.89	57.430	40.35
D465	7.2045	117.25	178.45	55.820	40.77
D466	7.6284	119.50	177.11	55.140	41.07
Y467	7.4901	119.72	176.87	56.670	39.93
R468	8.5465	121.50	179.35	55.488	29.378
E469	8.5993	124.54	177.48	57.500	29.05
E470	8.1258	117.00	176.03	56.670	27.58
S471	7.8779	116.97	176.11	57.850	65.97
E472	9.1528	123.72	174.98	59.510	26.71
E473	9.3119	120.70	179.55	59.690	26.93
Y474	7.6681	122.68	179.11	61.350	38.40
M475	8.0452	117.93	176.57	58.360	31.13
A476	7.9535	121.49	178.72	54.380	17.44
A477	7.5984	123.60	180.75	54.610	17.19
A478	8.8248	122.65	179.18	54.840	16.68
D479	7.9698	119.69	180.36	57.260	40.26
Y481	8.8520	122.52	178.05	61.470	36.339
N482	8.3625	117.04	176.98	55.979	37.748
R483	8.0735	122.83	178.14	59.544	29.618
L484	8.2503	121.69	179.55	57.510	41.19

K485	8.4378	120.33	177.23	59.280	30.59
Q486	7.6980	120.06	180.14	58.440	26.99
V487	7.8844	122.75	179.55	66.560	30.54
K488	7.9358	121.16	179.84	58.059	30.660
G489	7.3290	125.75	176.13	44.465	
S490	7.7486	118.18	174.39	58.270	65.71
A491	8.9447	125.82	174.81	54.791	17.287
D492	8.4740	118.59	180.74	57.570	39.80
Y493	7.6136	122.16	177.80	61.910	38.91
K494	7.9928	119.34	177.40	59.790	31.39
S495	8.4533	115.51	179.51	61.060	62.58
K496	7.9167	125.28	177.78	59.790	32.15
K497	8.5640	121.89	178.66	59.580	31.10
N498	8.2195	119.96	176.12	56.070	37.73
H499	8.5788	122.17	177.64	59.280	30.13
C500	8.5468	119.18	177.59	65.010	26.71
K501	7.7398	120.26	176.02	59.710	31.47
Q502	8.0507	119.67	175.96	59.320	28.68
L503	8.4952	121.35	178.38	57.680	40.10
K504	7.1106	116.74	177.87	57.290	39.82
S505	7.5081	115.01	179.33	61.320	62.84
K506	8.0697	126.16	176.90	59.540	29.10
L507	8.5360	118.13	179.21	57.577	39.659
S508	7.7778	114.58	176.97	56.318	39.882
H509	7.6930	122.89	174.63	58.028	
I510	8.3520	123.73	177.75	66.838	37.579
K511	8.3520	118.66	179.42	57.045	40.105
K512	7.6960	122.61	178.33	59.011	31.238
M513	8.2382	118.26	178.32	57.510	33.92
V514	8.5369	122.33	180.98	66.800	31.02
G515	8.3920	108.22	177.09	47.110	
D516	8.6808	122.61	176.94	56.900	39.95
Y517	7.5297	122.06	178.61	60.980	39.17
D518	8.6441	120.87	178.00	56.680	39.28
R519	7.7453	119.00	178.89	57.770	29.53
Q520	7.4993	118.18	177.36	56.070	28.34
K521	7.4893	121.61	176.16	55.990	31.56
T522	7.5766	121.33	179.34	63.180	70.62

* Protein at 180 μM, 25 °C, 10 mM sodium phosphate, pH 7.10, containing D_2O (10% volume) with 0.1% DSS.

Table S4. Chemical shifts for occludin 413-522

Residue	HN	N	CO	CA	CB
L410§	8.60	123.16	178.28	55.16	41.48
G411§	8.36	110.65	173.98		44.78
S412§	8.25	116.78	174.33	57.46	63.86
E413	8.42	122.94	176.85	57.18	28.87
E414	8.06	119.78	177.30	56.81	28.36
D415	7.77	121.00	177.70	55.09	39.71
W416	7.33	120.05	177.52	58.11	27.60
I423	8.40	124.60	177.31	61.57	37.89
T424	8.65	113.86	174.43	60.69	70.20
S425	7.18	116.09	174.03	57.34	66.44
D426	9.08	122.47		56.72	39.36
Q428	7.44	122.80	177.11	57.79	27.81
Q430	7.91	117.39	178.94	58.28	27.38
L431	7.55	122.97	178.83	57.90	40.57
Y432	8.76	122.44	178.15	60.52	35.72
K433	8.46	119.92	178.07	58.93	30.77
R434	8.10	120.43	179.49	59.22	28.90
N435	8.38	119.86	178.82	55.54	37.19
F436	9.04	125.34	175.54	61.06	38.04
D437	8.74	121.24	180.46	57.58	39.20
T438	8.33	116.26		65.64	68.25
G439	8.12	113.04	175.27	46.87	
L440	8.92	124.92	178.81	57.30	39.93
Q441	7.26	117.91	178.99	58.40	27.17
Y443	7.42	122.11	178.40	59.06	28.39
K444	8.75	121.18	180.47	60.96	37.82
S334	7.68	115.65	180.27	61.30	62.34
L446	7.93	124.78	178.62	57.21	41.80
Q447	8.74	119.49	178.87	57.75	27.24
S448	7.69	113.72	178.83	61.47	
E449	7.98	124.01	179.46	59.12	28.97
L450	8.52	121.27	178.17	41.51	
D451	8.30	119.36	178.17	57.13	41.41
E452	7.38	120.85	177.77	63.14	36.68
I453	7.22	119.43	177.85	57.83	29.11
N454	7.33	117.88	178.67	56.07	37.43
K455	8.60	123.37	178.29	55.05	41.12
E456	8.05	122.67	178.81	59.54	28.98
L457	8.21	120.97	178.95	58.48	40.93
S458	7.78	113.55		61.30	62.36
R459	8.46	123.04	176.78	57.23	28.84
L460	8.09	120.25	177.11	59.14	

D461	8.81	120.75		56.81	39.61
E463	7.86	121.39	178.87	59.18	28.32
L464	8.07	118.37			
D466	7.60	119.44	176.99	54.92	41.29
Y467	7.56	119.66		56.11	39.78
S471	7.86	116.77	174.92	57.83	65.66
E472	9.12	123.58	179.59	59.34	28.44
Y474	7.63	122.62	176.59	61.31	38.19
M475	8.04	117.83	178.86	58.28	30.84
A476	7.95	121.46	176.42	54.47	17.22
A477	7.56	123.44	179.18	57.61	16.77
A478	8.83	122.64	180.40	54.68	
D479	7.92	119.67	179.15	57.01	40.21
E480	7.65	122.54	178.21	58.26	28.39
Y481	8.87	122.36	177.02	61.47	38.04
N482	8.38	117.13	178.22	56.03	37.31
R483	8.04	122.51	179.61	59.51	29.11
L484	8.16	121.76	179.26	57.17	40.86
K485	8.45	121.33	180.28	58.69	30.48
Q486	7.67	120.02	179.53	58.03	27.09
V487	7.77	122.64	179.84	66.28	30.55
K488	7.91	121.37	176.08	58.03	30.55
G489	7.30	103.18	174.48	44.23	
S490	7.72	118.20	174.64	58.24	65.15
A491	8.88	125.28	180.82	54.76	17.17
D492	8.44	118.57	177.86	57.30	40.86
Y493	7.59	122.21	177.56	61.84	38.70
K494	8.06	119.02	179.69	59.95	31.20
S495	8.45	115.64	179.70	61.22	62.06
K496	7.87	125.42	178.69	59.73	32.00
K497	8.57	121.90	179.64	59.26	30.88
N498	8.20	119.31	177.67	56.11	37.69
H499	8.52	122.29	177.62	58.76	29.62
C500	8.48	118.56	176.25	64.82	26.30
K501	7.74	119.84	179.71	59.54	31.20
Q502	7.99	120.37	178.26	58.48	28.10
L503	8.51	121.57	178.13	57.14	41.54
K504	8.20	119.80	179.29	59.79	30.99
S505	7.46	115.59	178.85	61.22	62.34
K506	7.91	126.66	179.30	59.08	30.99
L507	8.54	118.38	179.30	57.50	39.42
S508	7.89	114.86		61.79	
H509	7.62	123.44	177.11	60.38	30.12
I510	8.24	120.10	177.77	66.91	37.55
K511	8.28	118.64	179.21	59.10	31.20

K512	7.69	122.88	178.33	58.87	30.93
M513	8.16	118.11	180.97	57.30	33.80
V514	8.40	122.13	177.14	66.68	31.00
G515	8.42	108.21	177.05	46.95	
D516	8.70	122.53	178.66	56.46	39.73
Y517	7.48	121.96	176.07	60.66	38.63
D518	8.62	120.89	178.97	56.44	38.98
R519	7.75	118.88	177.41	57.58	29.33
Q520	7.47	118.14	176.18	55.99	28.17
K521	7.47	121.63	176.04	55.87	31.35
T522	7.56	121.35	179.33	63.06	70.27

[§]Residues 410-412 represent a synthetic N-terminal extension and are not native occludin sequence.

* Protein at 180 μM, 25 °C, 10 mM sodium phosphate, pH 7.10, containing D_2O (10% volume) with 0.1% DSS.

SI References

1. Raleigh DR*, et al.* (2011) Occludin S408 phosphorylation regulates tight junction protein interactions and barrier function *J Cell Biol* 193:565-582.
2. Pace CN, Vajdos F, Fee L, Grimsley G, & Gray T (1995) How to measure and predict the molar absorption coefficient of a protein *Protein Sci.* 4:2411-2423.
3. Chen YH, Yang JT, & Chau KH (1974) Determination of the helix and beta form of proteins in aqueous solution by circular dichroism *Biochemistry* 13:3350-3359.
4. Czisch M & Boelens R (1998) Sensitivity enhancement in the TROSY experiment *J. Magn. Reson.* 134:158-160.
5. Schulte-Herbruggen T, Briand J, Meissner A, & Sorensen OW (1999) Spin-state-selective TPPI: a new method for suppression of heteronuclear coupling constants in multidimensional NMR experiments *J. Magn. Reson.* 139:443-446.
6. Pervushin KV, Wider G, & Wuthrich K (1998) Single Transition-to-single Transition Polarization Transfer (ST2-PT) in [15N,1H]-TROSY *J. Biomol. NMR* 12:345-348.
7. Weigelt J (1998) Single Scan, Sensitivity- and Gradient-Enhanced TROSY for Multidimensional NMR Experiments *J. Am. Chem. Soc.* 120:10778-10779.
8. Loria JP, Rance M, & Palmer AG, 3rd (1999) Transverse-relaxation-optimized (TROSY) gradient-enhanced triple-resonance NMR spectroscopy *J. Magn. Reson.* 141:180-184.
9. Rance M, Loria JP, & Palmer AGr (1999) Sensitivity improvement of transverse relaxation-optimized spectroscopy *J. Magn. Reson.* 136:92-101.
10. Zhu G, Kong XM, & Sze KH (1999) Gradient and sensitivity enhancement of 2D TROSY with water flip-back, 3D NOESY-TROSY and TOCSY-TROSY experiments *J. Biomol. NMR* 13:77-81.
11. Schulte-Herbruggen T & Sorensen OW (2000) Clean TROSY: compensation for relaxation-induced artifacts *J. Magn. Reson.* 144:123-128.
12. Fernandez C, Adeishvili K, & Wuthrich K (2001) Transverse relaxation-optimized NMR spectroscopy with the outer membrane protein OmpX in dihexanoyl phosphatidylcholine micelles *Proc. Natl. Acad. Sci. U.S.A.* 98:2358-2363.
13. Eletsky A, Kienhofer A, & Pervushin K (2001) TROSY NMR with partially deuterated proteins *J. Biomol. NMR* 20:177-180.
14. Salzmann M, Pervushin K, Wider G, Senn H, & Wüthrich K (2000) NMR Assignment and Secondary Structure Determination of an Octameric 110 kDa Protein Using TROSY in Triple Resonance Experiments *J. Am. Chem. Soc.* 122:7543-7548.
15. Salzmann M, Wider G, Pervushin K, & Wuthrich K (1999) Improved sensitivity and coherence selection for [15N,1H]-TROSY elements in triple resonance experiments *J. Biomol. NMR* 15:181-184.

16. Hansen AL*, et al.* (2021) 2D NMR-Based Metabolomics with HSQC/TOCSY NOAH Supersequences *Anal. Chem.* 93:6112-6119.
17. Kay L, Keifer P, & Saarinen T (2002) Pure absorption gradient enhanced heteronuclear single quantum correlation spectroscopy with improved sensitivity *J. Am. Chem. Soc.* 114:10663-10665.
18. Schleucher J*, et al.* (1994) A general enhancement scheme in heteronuclear multidimensional NMR employing pulsed field gradients *J. Biomol. NMR* 4:301-306.
19. Skrynnikov NR, Dahlquist FW, & Kay LE (2002) Reconstructing NMR spectra of "invisible" excited protein states using HSQC and HMQC experiments *J. Am. Chem. Soc.* 124:12352-12360.
20. Delaglio F*, et al.* (1995) NMRPipe: a multidimensional spectral processing system based on UNIX pipes *J. Biomol. NMR* 6:277-293.
21. Keller R & Wuthrich K (2004) Computer-aided resonance assignment (CARA). (http://www.nmr.ch).
22. Zhu G, Xia Y, Nicholson LK, & Sze KH (2000) Protein dynamics measurements by TROSY-based NMR experiments *J. Magn. Reson.* 143:423-426.
23. Hwang T-L, Mori S, Shaka AJ, & van Zijl PCM (1997) Application of Phase-Modulated CLEAN Chemical EXchange Spectroscopy (CLEANEX-PM) to Detect Water−Protein Proton Exchange and Intermolecular NOEs *J. Am. Chem. Soc.* 119:6203-6204.
24. Hwang TL, van Zijl PC, & Mori S (1998) Accurate quantitation of water-amide proton exchange rates using the phase-modulated CLEAN chemical EXchange (CLEANEX-PM) approach with a Fast-HSQC (FHSQC) detection scheme *J. Biomol. NMR* 11:221-226.
25. Grzesiek S & Bax A (2002) The importance of not saturating water in protein NMR. Application to sensitivity enhancement and NOE measurements *J. Am. Chem. Soc.* 115:12593-12594.
26. Williamson MP (2013) Using chemical shift perturbation to characterise ligand binding *Prog Nucl Magn Reson Spectrosc* 73:1-16.
27. Clore GM & Iwahara J (2009) Theory, practice, and applications of paramagnetic relaxation enhancement for the characterization of transient low-population states of biological macromolecules and their complexes *Chem. Rev.* 109:4108-4139.
28. Fawzi NL, Ying J, Torchia DA, & Clore GM (2012) Probing exchange kinetics and atomic resolution dynamics in high-molecular-weight complexes using dark-state exchange saturation transfer NMR spectroscopy *Nat Protoc* 7:1523-1533.
29. Sjodt M & Clubb RT (2017) Nitroxide Labeling of Proteins and the Determination of Paramagnetic Relaxation Derived Distance Restraints for NMR Studies *Bio Protoc* 7.
30. Marchiando AM*, et al.* (2010) Caveolin-1-dependent occludin endocytosis is required for TNF-induced tight junction regulation in vivo *J Cell Biol* 189:111-126.

31. Kuo WT*, et al.* (2019) Inflammation-induced Occludin Downregulation Limits Epithelial Apoptosis by Suppressing Caspase-3 Expression *Gastroenterol.* 157:1323-1337.
32. Yu D*, et al.* (2010) MLCK-dependent exchange and actin binding region-dependent anchoring of ZO-1 regulate tight junction barrier function *Proc. Natl. Acad. Sci. U.S.A.* 107:8237-8241.
33. Nusrat A*, et al.* (2000) The coiled-coil domain of occludin can act to organize structural and functional elements of the epithelial tight junction *J. Biol. Chem.* 275:29816-29822.
34. Walter JK*, et al.* (2009) Redox-sensitivity of the dimerization of occludin *Cell. Mol. Life Sci.* 66:3655-3662.
35. Walter JK*, et al.* (2009) The oligomerization of the coiled coil-domain of occludin is redox sensitive *Ann. N. Y. Acad. Sci.* 1165:19-27.